Acta Crystallographica Section F
Structural Biology and Crystallization Communications
ISSN 1744-3091

Expression, purification, crystallization and preliminary X-ray diffraction analysis of the VP8* sialic acid-binding domain of porcine rotavirus strain OSU

Yang-De Zhang,[a]* Hao Li,[a] Hui Liu[b] and Yi-Feng Pan[b]

[a]National Hepatobiliary and Enteric Surgery Research Center of The Ministry of Health, Xiangya Hospital, Central South University, Hunan Province, People's Republic of China, and [b]Biochemistry Laboratory, Institution of Biomedical Engineering, Central South University, Hunan Province, People's Republic of China

Correspondence e-mail: zhangyd1960@yahoo.com.cn

Received 22 October 2006
Accepted 22 December 2006

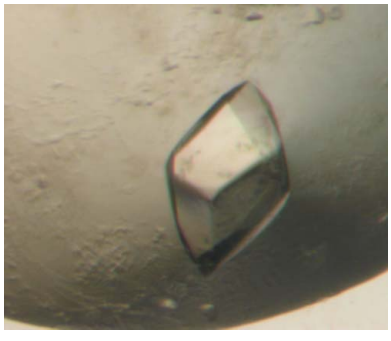

The rotavirus outer capsid spike protein VP4 is utilized in the process of rotavirus attachment to and membrane penetration of host cells. VP4 is cleaved by trypsin into two domains: VP8* and VP5*. The VP8* domain is implicated in initial interaction with sialic acid-containing cell-surface carbohydrates and triggers subsequent virus invasion. The VP8* domain from porcine OSU rotavirus was cloned and expressed in *Escherichia coli*. Different crystal forms (orthorhombic $P2_12_12_1$ and tetragonal $P4_12_12$) were harvested from two distinct crystallization conditions. Diffraction data have been collected to 2.65 and 2.2 Å resolution and the $VP8^*_{65–224}$ structure was determined by molecular replacement.

1. Introduction

Rotaviruses are recognized as the major aetiological agent of severe dehydrating diarrhoea in the young of humans and other animal species worldwide, accounting for an estimated 500 000 deaths each year (Parashar *et al.*, 2003). The mature rotavirus virion is a triple-layered particle (TLP) comprised of three concentric layers of proteins that encompass a double-stranded RNA genome (Estes, 2001). The innermost layer is formed by the VP2 protein, which surrounds the viral genome and two viral enzymes, VP1 and VP3. The intermediate layer is formed by the VP6 protein, which lies on top of VP2 to form a double-layered particle (DLP). The outermost layer of the virion is composed of two proteins: the coat glycoprotein VP7, forming the smooth surface of the virus, and the spike-like protein VP4, which projects from the virus surface (Shaw *et al.*, 1993). Unlike non-infectious DLP, the infectious TLP binds to gangliosides, suggesting that the outermost layer proteins play a role in oligosaccharide binding (Delorme *et al.*, 2001). Furthermore, both VP4 and VP7 are involved in interactions of rotavirus with its host-cell receptors and cell penetration (Sanchez-San Martin *et al.*, 2004). Proteolytic cleavage of VP4 by trypsin is associated with virion penetration into the cell interior and increased infectivity, producing an N-terminal fragment VP8* and a C-terminal fragment VP5* (Ruggeri & Greenberg, 1991; Estes *et al.*, 1981). In some rotavirus strains VP8* is considered to be a carbohydrate-binding domain which mediates initial cell attachment by recognizing a sialic acid (SA) containing glycoconjugate (Dormitzer *et al.*, 2004; Fiore *et al.*, 1991). In fact, that infectivities of some animal rotavirus strains are dependent on the presence of SA-containing compounds on the host-cell surface; the infectivity is significantly decreased by neuraminidase (NA) treatment of the cells (Yolken *et al.*, 1987). These animal rotavirus strains are termed NA-sensitive strains. Unlike these strains, most human rotavirus strains are NA-insensitive (Ciarlet & Estes, 1999; Ciarlet *et al.*, 2002). Although the importance of SA in the infectivity of these NA-insensitive strains is still to be characterized, this does not rule out the possibility that these NA-insensitive strains do not need SA for cell attachment. Indeed, it has been reported that human rotavirus strains were able to recognize internal SA within oligosaccharides (Guo *et al.*, 1999; Guerrero *et al.*, 2000).

Rotavirus infections indicate significant host-specificity, which challenges vaccine development. To date, commercially available

vaccines have only been designed for the four common VP7 serotypes (G1–G4) and the VP4 serotype (G8). However, increasing numbers of cases of other unconventional serotypes have been reported (Feeney *et al.*, 2006). Given the fact that the VP4 protein is involved in cell-recognition processes, the VP8* carbohydrate-binding domain is therefore considered to be a promising drug-design target. Only a few studies have reported structural information on the VP8* domain (Kraschnefski *et al.*, 2005; Dormitzer *et al.*, 2002; Scott *et al.*, 2005; Monnier *et al.*, 2006). Here, we report the cloning, expression, purification and structure determination of VP8$^{*}_{65–224}$ from the NA-sensitive porcine rotavirus strain OSU.

2. Materials and methods

2.1. Cloning and expression

To construct the plasmid pGex-OSU-VP8$^{*}_{65–224}$, the nucleotide sequence encoding OSU-VP8$^{*}_{65–224}$ was cloned between the *Bam*HI and *Eco*RI restriction sites of vector pGex-4T-1 (Amersham Biosciences) with an in-frame N-terminal GST. The integrity of the VP8* gene fragment was assessed by DNA sequencing. The predicted amino-acid sequence of pGex-OSU-VP8$^{*}_{65–224}$ was identical to the published OSU VP4 sequence except for serine substituting alanine at position 184 (accession No. X13190, NCBI, NIH). It is noteworthy that the vector sequence immediately preceding the OSU-VP8$^{*}_{65–224}$ N-terminus is **Arg**-Gly-Ser, which contains a trypsin cleavage site (indicated in bold). Hence, the predicted N-terminus of the final construct may contain two additional amino acids, glycine and serine; however, verification of this assumption will have to await completion of the refinement. *Escherichia coli* strain BL21 DE3 transformed with the pGex-OSU-VP8$^{*}_{65–224}$ plasmid was grown at 310 K in Luria–Bertani (LB) medium supplemented with 100 µg ml^{-1} ampicillin. After reaching an A_{600} of 0.6, the cultures were incubated at 298 K for 1 h and isopropyl β-D-thiogalactoside (IPTG) was then added to a final concentration of 1 m*M*. Cells were harvested 4 h after induction and frozen.

2.2. Purification

Frozen cell pellets were thawed in 137 m*M* NaCl, 2.7 m*M* KCl, 10 m*M* Na_2HPO_4, 2 m*M* KH_2PO_4 pH 7.3 (PBS) supplemented with 1% Triton X-100 and 1 m*M* phenylmethylsulfonyl fluoride (PMSF). The suspension was sonicated and cell debris was removed by centrifugation at 20 000*g* for 1 h. The supernatant was passed over a glutathione Sepharose column (Amersham-Pharmacia Biotech) and the column was then washed with 20 m*M* Tris pH 8.0, 100 m*M* NaCl, 1 m*M* $CaCl_2$ (TNC). Digestion was performed by adding TPCK-treated trypsin (Worthington Biochemical) to a final concentration of 5 µg ml^{-1} following by 2 h incubation at room temperature. The cleaved protein was eluted with TNC and the eluant was passed over a benzamidine Sepharose column (Amersham Pharmacia Biotech) pre-equilibrated with TNC. The protein was then concentrated using an Amicon Ultrapure-15 centrifugal filter device (5 kDa molecular-weight cutoff, Millipore) and subjected to size-exclusion chromatography over a Superdex 75 column (Amersham Pharmacia Biotech) equilibrated in 20 m*M* Tris pH 8.0, 100 m*M* NaCl, 1 m*M* EDTA. Purified protein was analysed for homogeneity by SDS–PAGE analysis (Fig. 1). Approximately 11 mg of purified protein was obtained from 1 l culture.

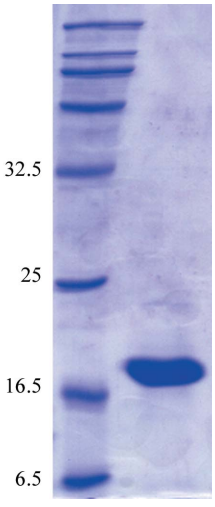

Figure 1
SDS–PAGE analysis of OSU VP8$^{*}_{65–224}$. Lane 1 contains molecular-weight markers (kDa) and lane 2 contains protein sample (50 µg was loaded; the calculated MW is 18 095 Da).

2.3. Crystallization and data collection

Crystallization trials were performed in the absence and presence of 2-*O*-methyl-α-D-*N*-acetylneuraminic acid (Neu5Acα2Me) using the sitting-drop vapour-diffusion method with Crystal Screen kits (Hampton Research) at 293 K. Crystals formed under two conditions, one of which produced a crystal in the absence of Neu5Acα2Me and the other of which produced a crystal in the presence of Neu5Acα2Me. In the absence of Neu5Acα2Me, crystals (Fig. 2) formed within one week from a sample solution containing 30 mg ml^{-1} OSU VP8$^{*}_{65–224}$, 5.6 m*M* Tris–HCl pH 8.0, 16 m*M* sodium phosphate pH 7.0, 35 m*M* NaCl, 0.3 m*M* EDTA mixed with an equal volume of a reservoir solution containing 2 *M* ammonium sulfate, 3% PEG 400 and 100 m*M* PIPES pH 6.5 (developed from a condition described previously by Dormitzer *et al.*, 2002). In the presence of Neu5Acα2Me, 10 mg ml^{-1} OSU VP8$^{*}_{65–224}$ was premixed with sialoside at a concentration of 31 m*M*, giving a protein:ligand ratio of 1:50. Rod-shaped crystals (Fig. 3) formed overnight from combination of an equal volume of the premixed sample solution and reservoir solution containing 70% MPD, 0.1 *M* HEPES pH 7.5 (a condition described previously by Scott *et al.*, 2005).

Data sets were collected from the two crystal forms to 2.65 and 2.2 Å, respectively, at room temperature (295 K) on a MacScience

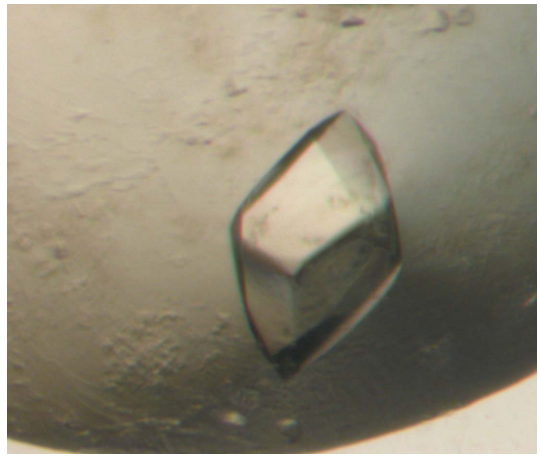

Figure 2
Crystal of OSU VP8$^{*}_{65–224}$ grown in the absence of Neu5Acα2Me. Typical crystal dimensions are 230 × 230 × 110 µm.

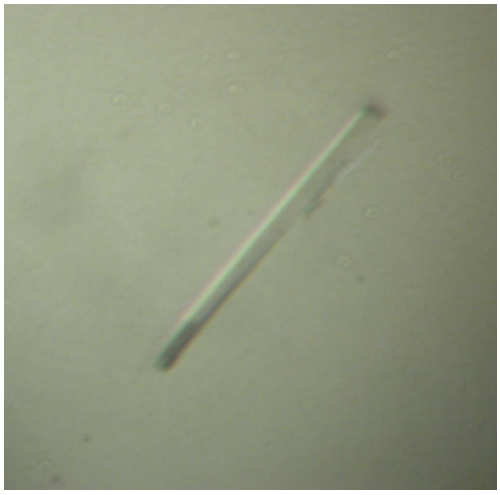

Figure 3
Crystal of OSU VP8*$_{65–224}$ grown in the presence of Neu5Acα2Me. Typical crystal dimensions are 20 × 20 × 380 µm.

DIP2020 imaging plate mounted on an Elliot GX21 rotating-anode generator producing Cu $K\alpha$ radiation. Data were reduced and scaled using the program *XDS* (Kabsch, 1988) and programs from the Groningen *BIOMOL* software package. For the purposes of molecular replacement, a homology model of porcine OSU VP8*$_{65–224}$ was built using *MODELLER* (Sali & Blundell, 1993) on the basis of amino-acid sequence alignment with rhesus RRV VP8* (72% amino-acid sequence identity). Molecular replacement was performed using *AMoRe* (Navaza, 1994).

X-ray diffraction data were collected to 2.65 Å (Table 1) from a crystal grown in the absence of Neu5Acα2Me. The crystal contains one molecule in the asymmetric unit of the tetragonal system ($P4_12_12$), with a solvent content of 55.2% (V_M = 2.8 Å^3 Da^{-1}). Molecular replacement in the resolution range 15–3 Å gave a highest rotation-function peak with an R factor of 53.8% and a correlation coefficient of 19.6%, which were distinct from the next highest peak, which had an R factor of 55.2% and a correlation coefficient of 17.8%. The translation function gave the best solution with an an R factor of 48.5% and a correlation coefficient of 39.8%, which were clearly above the next solution, which had an R factor of 51.9% and a correlation coefficient of 27.3%. Rigid-body refinement gave an R factor of 45.6% and a correlation coefficient of 42.9%.

X-ray diffraction data were collected to 2.2 Å (Table 1) from a crystal grown in the presence of Neu5Acα2Me. The crystal contains two molecules in the asymmetric unit of the orthorhombic system ($P2_12_12_1$), with a solvent content of 53.8% (V_M = 3.3 Å^3 Da^{-1}). Molecular replacement in the resolution range 8–3 Å gave a highest rotation-function peak with an R factor of 51.6% and a correlation coefficients of 21.3%, which were distinct from the next highest peak, which had an R factor of 54.5% and a correlation coefficient of 18.6%. The translation function gave the best solution with an R factor of 46.3% and a correlation coefficient of 40.5%, which were clearly above the next solution, which had an R factor of 48.7% and a correlation coefficient of 36.2%. After fixing the top solution, rigid-body refinement was applied and the translation function was calculated for the remaining top ten solutions. An R factor of 42.6% and a correlation coefficient of 45.1% were obtained for the second molecule in the asymmetric unit. Rigid-body refinement was applied to these two molecules and a clear solution was obtained with an R factor of 39.6% and a correlation coefficient of 48.9%.

Table 1
Summary of data-collection statistics for OSU VP8*$_{65–224}$.

Values in parentheses are for the highest resolution shell.

	Crystal grown in the absence of Neu5Acα2Me	Crystal grown in the presence of Neu5Acα2Me
Space group	$P4_12_12$	$P2_12_12_1$
Unit-cell parameters (Å, °)	$a = b = 49.82$, $c = 129.65$, $\alpha = \beta = \gamma = 90$	$a = 54.31$, $b = 60.23$, $c = 110.78$, $\alpha = \beta = \gamma = 90$
Resolution limits (Å)	30–2.65 (2.81–2.65)	28–2.2 (2.31–2.2)
No. of observations	20056 (1668)	58766 (3982)
No. of unique observations	5688 (824)	12744 (1022)
Average redundancy	3.53 (2.02)	4.61 (3.9)
Completeness (%)	92.8 (91.5)	90.6 (88.2)
$\langle I/\sigma(I)\rangle$	8.1 (3.5)	5.9 (2.6)
R_{merge} (%)	11.2 (32.6)	10.5 (28.9)

3. Conclusions

Porcine OSU VP8*$_{65–224}$ has been successfully cloned, expressed, purified and crystallized in the absence and presence of 2-*O*-methyl-α-D-*N*-acetylneuraminic acid. Refinement of the models is in progress. Work is also in progress to produce crystals of better diffraction quality.

This work was supported in part by a grant from the National Key Technologies R&D Program, No. (863)2002AA214011, and the National Basic Research Program, No. (863)2003AA217020, of the Ministry of Science and Technology, People's Republic of China.

References

Ciarlet, M. & Estes, M. K. (1999). *J. Gen. Virol.* **80**, 943–948.
Ciarlet, M., Ludert, J. E., Iturriza-Gomara, M., Liprandi, F., Gray, J. J., Desselberger, U. & Estes, M. K. (2002). *J. Virol.* **76**, 4087–4095.
Delorme, C., Brussow, H., Sidoti, J., Roche, N., Karlsson, K. A., Neeser, J. R. & Teneberg, S. (2001). *J. Virol.* **75**, 2276–2287.
Dormitzer, P. R., Nason, E. B., Prasad, B. V. & Harrison, S. C. (2004). *Nature (London)*, **430**, 1053–1058.
Dormitzer, P. R., Sun, Z. Y., Wagner, G. & Harrison, S. C. (2002). *EMBO J.* **21**, 885–897.
Estes, M. K. (2001). *Fields Virology*, 4th ed., edited by D. M. Knipe & P. M. Howley, p. 1747. Philadelphia: Lippincott–Raven.
Estes, M. K., Graham, D. Y. & Mason, B. B. (1981). *J. Virol.* **39**, 879–888.
Feeney, S. A., Mitchell, S. J., Mitchell, F., Wyatt, D. E., Fairley, D., McCaughey, C., Coyle, P. V. & O'Neill, H. J. (2006). *J. Med. Virol.* **78**, 1119–1123.
Fiore, L., Greenberg, H. B. & Mackow, E. R. (1991). *Virology*, **181**, 553–563.
Guerrero, C. A., Zarate, S., Corkidi, G., Lopez, S. & Arias, C. F. (2000). *J. Virol.* **74**, 9362–9371.
Guo, C. T., Nakagomi, O., Mochizuki, M., Ishida, H., Kiso, M., Ohta, Y., Suzuki, T., Miyamoto, D., Hidari, K. I. & Suzuki, Y. (1999). *J. Biochem. (Tokyo)*, **126**, 683–688.
Kabsch, W. (1988). *J. Appl. Cryst.* **21**, 916–924.
Kraschnefski, M. J., Scott, S. A., Holloway, G., Coulson, B. S., von Itzstein, M. & Blanchard, H. (2005). *Acta Cryst.* F**61**, 989–993.
Monnier, N., Higo-Moriguchi, K., Sun, Z. Y., Prasad, B. V., Taniguchi, K. & Dormitzer, P. R. (2006). *J. Virol.* **80**, 1513–1523.
Navaza, J. (1994). *Acta Cryst.* A**50**, 157–163.
Parashar, U. D., Hummelman, E. G., Bresee, J. S., Miller, M. A. & Glass, R. I. (2003). *Emerg. Infect. Dis.* **9**, 565–572.
Ruggeri, F. M. & Greenberg, H. B. (1991). *J. Virol.* **65**, 2211–2219.
Sali, A. & Blundell, T. L. (1993). *J. Mol. Biol.* **234**, 779–815.
Sanchez-San Martin, C., Lopez, T., Arias, C. F. & Lopez, S. (2004). *J. Virol.* **78**, 2310–2318.
Scott, S. A., Holloway, G., Coulson, B. S., Szyczew, A. J., Kiefel, M. J., von Itzstein, M. & Blanchard, H. (2005). *Acta Cryst.* F**61**, 617–620.
Shaw, A. L., Rothnagel, R., Chen, D., Ramig, R. F., Chiu, W. & Prasad, B. V. (1993). *Cell*, **74**, 693–701.
Yolken, R. H., Willoughby, R., Wee, S. B., Miskuff, R. & Vonderfecht, S. (1987). *J. Clin. Invest.* **79**, 148–154.